Controllable optical bistability in photonic-crystal one-atom laser

Xiao-yong Guo and Shu-chen Lü*

Heilongjiang Key Laboratory for Advanced Functional Material and Excited State Process, School of Physics and Electronic Engineering, Harbin Normal University, Harbin 150025, China

(Received 24 March 2009; published 21 October 2009)

We investigate the property of optical bistability in a photonic-crystal one-atom laser when nonlinear microcavity is present. The physical system consists of a coherently driven two-level light emitter strongly coupled to a high-quality microcavity which is embedded within a photonic crystal and another coherent probing field which has incident into the microcavity. In our case, the microcavity is fabricated by nonlinear material and placed as an impurity in photonic crystal. This study reveals that such a system can exhibit optical bistability. The dependence of threshold value and hysteresis loop on the photonic band gap of the photonic crystal, driving field Rabi frequency and dephasing processes, are studied. Our results clearly illustrate the ability to control optical bistability through suitable photonic-crystal architectures and external coherent driving field, and this study suggests that in a photonic-crystal nonlinear microcavity, the one-atom laser acts as an effective controllable bistable device in the design of all-light digital computing systems in the near future.

DOI: 10.1103/PhysRevA.80.043826 PACS number(s): 42.65.Pc, 42.55.Tv

I. INTRODUCTION

The character of bistable system is that there are two stable output intensities for a single input intensity [1]. In the past few decades, optical bistability has inspired considerable investigation due to its significant applications in photon control devices [2–8]. It is well know that superior optical bistable device requires the materials with large nonlinear refractive index coefficient and fast speed nonlinear response. Unfortunately, it is quite difficult to select an appropriate nonlinear material and the physical parameters of the material cannot be manipulated arbitrarily. So how to control bistability artificially has attracted a lot of interest in this research region. Up to now, many approaches have been proposed such as introducing a strong electromagnetic field [9,10], via spontaneously generated coherence in an atom system [11], and applying photonic band-gap (PBG) structures [12–14].

Recently, there is much interest in one-atom laser. Such a system is one of the key to study quantum effects in the interaction of electromagnetic fields with matter [15–19]. The so-called photonic-crystal one-atom laser is only one atom or quantum dot interacting with the quantized field of a photonic-crystal microcavity. It is well known that in the photonic crystal there is a periodicity in the refraction index which produces the scattering of light outside of the crystal for certain frequencies related to the refraction index periodicity [20]. Consequently, those modes are absent from the crystal so that a gap is formed. This property produces new optical phenomenon, such as photon-atom bound states [21], fractionalized single-atom inversion [22], coherent control of spontaneous emission through quantum interference [23], optical bistability, and switching in multiatom systems [24]. By embedding a point defect in the periodic structure, a single isolated band may occur inside the gap and electromagnetic modes (defect modes) are localized in the vicinity of the defect [20,25]. This defect structure is the photonic-crystal microcavity. From 2004 to 2008, Florescu *et al.* [26–29] published a series of papers to propose a detailed quantum theory of a one-atom laser in photonic-crystal microcavity. According to the theory, a wide variety of novel quantum statistical and spectral features have been unveiled. In particular, better coherence, strong enhancement of the cavity field, and photon antibunching have been predicted. Following the progress in experimental techniques, some of them are verified experimentally [30–34].

In this paper, we investigate property of optical bistability in a photonic-crystal one-atom laser when nonlinear material is present. The photonic-crystal microcavity is a point defect embedded within periodic dielectric structures. Within a full band gap, photons will be completely localized in the vicinity of the defect [25]. Therefore, there is no fundamental upper boundary to the microcavity Q factor (quality factor) [28]. In the previous theoretical study of one-atom laser in photonic crystal, the microcavity is considered to be fabricated by linear dielectric material, but in our study the microcavity is considered to be fabricated by nonlinear material. The physical system consists of a coherently driven two-level light emitter strongly coupled to a high-quality microcavity. The microcavity is made of a photonic crystal with a nonlinear defect and another coherent probing field which has incident into the microcavity. By the dressed-atom approach and Born-Markov approximation, we obtained the master equation for the system which is atom plus cavity field and then we derived the analytical expression for the correlation between cavity field amplitude and incident coherent probing field intensity via an appropriate approximation. The numerical simulation has shown that under suitable physical conditions, the system can produce optical bistability and how the bistable properties vary with the controllable parameters of the system.

The outline of this paper is as follows. In Sec. II, we present the model Hamiltonian and derive the master equation for the system. In Sec. III, we derive the equations of motion for expectation values of atomic and cavity field operators and the steady-state solutions are obtained under

*Corresponding author; lushuchen63@yahoo.com.cn

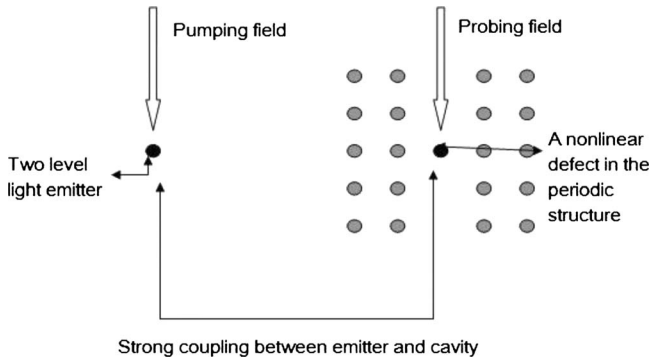

FIG. 1. The system under consideration consists of a coherently driven two-level light emitter strongly coupled to a high-quality nonlinear microcavity which is embedded within a photonic crystal and another coherent probing field which has incident into the microcavity.

small fluctuation approximation. Then we define the bistable state equations of system and derive its analytical expression. In Sec. IV, we investigate the bistable properties with different physical parameters. Finally, we summarized the results in Sec. V.

II. MASTER EQUATION

Let us consider a single two-level light emitter (atom or quantum dot) with ground state $|1\rangle$ and excited state $|2\rangle$ separated by the transition frequency ω_a. The atom is coupled to a single mode of a high-Q microcavity with coupling constant g and is driven by a coherent external laser field of a frequency ω_L and the resonant Rabi frequency (intensity) ε. The Rabi frequency characterizes the strength of the driving field and is proportional to the product of the absolute value of atomic dipole moment d_{12} and the driving field amplitude E ($\varepsilon = d_{12}|E|/\hbar$). The microcavity is embedded within photonic crystal as a nonlinear impurity and the cavity mode frequency is ω_c. The system under consideration is schematically depicted in Fig. 1. For simplicity, we treat the driving external field classically and work in the interaction picture. Under the electric-dipole and the rotating-wave approximations, the total system is described by a Hamiltonian which can be written as

$$H = H_0 + H_1 + H_2 + H_{dephase} + H_{damping}. \tag{1}$$

In Eq. (1), the first term H_0 is the noninteracting Hamiltonian of the driven atom plus the cavity mode plus the photonic-crystal radiation reservoir modes and the H_0 is given as

$$H_0 = \frac{1}{2}\hbar\Delta_a\sigma_3 + \hbar\varepsilon(\sigma_{12} + \sigma_{21}) + \hbar\Delta_c a^\dagger a + \hbar\sum_\lambda \Delta_\lambda a_\lambda^\dagger a_\lambda, \tag{2}$$

where a and $a^\dagger$ are the cavity mode annihilation and creation operators, respectively, a_λ and $a_\lambda^\dagger$ are the photonic-crystal radiation reservoir annihilation and creation operators, $\sigma_{ij} = |i\rangle\langle j|$ $(i,j=1,2)$ are the bare-atomic operators, $\sigma_3 = \sigma_{22} - \sigma_{11}$ describes the bare-atomic inversion, and $\Delta_a = \omega_a - \omega_L$, $\Delta_c = \omega_c - \omega_L$, and $\Delta_\lambda = \omega_\lambda - \omega_L$ are the detuning of the atomic resonance frequency ω_a, of the cavity mode frequency ω_c, of the frequency ω_λ of a mode λ of the photonic-crystal radiation reservoir, respectively. The second term H_1 in Eq. (1) describes the nonlinear effect of microcavity [35] and the incident of coherent probing field of a frequency ω_i and the Rabi frequency ξ and the H_1 is given as

$$H_1 = \hbar\chi a^\dagger a^\dagger a a + i\hbar\xi(a^\dagger e^{-i\Delta_i t} - a e^{i\Delta_i t}), \tag{3}$$

where $\Delta_i = \omega_i - \omega_L$ is the detuning of incident probing field frequency ω_i and χ is the dispersive part of third-order nonlinear polarizability of nonlinear material [35]. In our model, χ describes the strength of nonlinear effect in the cavity. For simplicity, we also treat the probing field classically. The third term

$$H_2 = i\hbar g(\sqrt{a^\dagger a}\, a^\dagger \sigma_{12} - a\sqrt{a^\dagger a}\,\sigma_{21}) + i\hbar\sum_\lambda g_\lambda(a_\lambda^\dagger \sigma_{12} - \sigma_{21} a_\lambda) \tag{4}$$

is the interaction Hamiltonian between the atom and the cavity mode as well as the photonic-crystal vacuum radiation modes. In particular, the strength of the coupling between atom and cavity mode is proportional to the cavity field amplitude which reflects the nonlinear interactions. In Eq. (4), the coupling constant between the atom and the cavity mode is given by $g = (\omega_a d_{21}/\hbar)(\hbar/2\varepsilon_0\omega_c V)^{1/2}\hat{e}\cdot\hat{u}_d$, where d_{21} and $\hat{u}_d$ are the absolute value and the unit vector of the atomic dipole moment respectively, V is the volume of the cavity mode, $\hat{e}$ is the polarization mode of the cavity radiation field, ε_0 is the dielectric constant, and g_λ is the coupling constant between the atom and the mode λ of the radiation field of the photonic reservoir. Both g and g_λ are taken as positive real numbers.

The Hamiltonian $H_{dephase}$ describes additional dephasing interactions, which may arise from scattering phonons of the host crystal on the atom embedded in the solid part of the dielectric material. For simplicity, assume that the phonon density of states (DOS) is broad and displays no sharp features. In this case, $H_{dephase}$ contributes one term to the master equation of the system [36]

$$\left(\frac{\partial\rho}{\partial t}\right)_{dephase} = \gamma_p(\sigma_3\rho\sigma_3 - \rho), \tag{5}$$

where γ_p is a phenomenological dephasing rate.

The Hamiltonian $H_{damping}$ describes the damping of the cavity field. In our case, this may arise from infinitesimal asymmetry of the defect architecture (caused by the manufacturing process) that allows weak direct coupling between the vacuum modes and the microcavity mode within the PBG [26,37]. Also, a small amount of light can be emitted in the vicinity of the microcavity. The contribution of this type of damping to the master equation is expressed as

$$\left(\frac{\partial\rho}{\partial t}\right)_{damping} = \kappa(2a\rho a^\dagger - a^\dagger a\rho - \rho a^\dagger a), \tag{6}$$

where κ is the phenomenological cavity decay rate. The cavity quality factor is then defined as $Q \equiv \omega_c/\kappa$.

As a matter of fact, the strong pumping field can drive the atom to form dressed atom before the spontaneous emission ,taking place. Hence, the electromagnetic field is considered to be interaction with dressed atom. In order to describe this interaction, it is useful to transform Eq. (1) from bare-atom representation to dressed-atom representation by introducing the dressed states [29]. The so-called dressed states are the eigenstates of atom plus pump field noninteracting Hamiltonian H_{af} as given below

$$H_{af} = \frac{1}{2}\hbar\Delta_a\sigma_3 + \hbar\varepsilon(\sigma_{12} + \sigma_{21}). \tag{7}$$

Since the driving field is treated classically, the eigenstates of Eq. (7) can be easily found

$$|\tilde{1}\rangle = c|1\rangle - s|2\rangle, \tag{8a}$$

$$|\tilde{2}\rangle = s|1\rangle + c|2\rangle. \tag{8b}$$

Here $c \equiv \cos(\phi)$, $s \equiv \sin(\phi)$, and angle ϕ is in the interval $[0, \pi]$ and is defined by

$$\cos^2(\phi) = \frac{1}{2}\left(1 + \frac{\Delta_a}{\Omega}\right), \tag{9}$$

where $\Omega = \sqrt{4\varepsilon^2 + \Delta_a^2}$ is the generalized Rabi frequency.

By the Eq. (8), we can obtain the relationship between bare-atomic operators and the dressed-state atomic operators

$$\sigma_{12} = \frac{1}{2}\sin(2\phi)R_3 - \sin^2\phi R_{21} + \cos^2\phi R_{12}, \tag{10a}$$

$$\sigma_3 = \sigma_{22} - \sigma_{11} = \cos(2\phi)R_3 - \sin(2\phi)(R_{12} + R_{21}), \tag{10b}$$

$$R_3 = R_{22} - R_{11}, \tag{10c}$$

where $R_{ij} = |\tilde{i}\rangle\langle\tilde{j}|$ $(\tilde{i}, \tilde{j} = 1, 2)$ are the dressed-state atomic operators. Under the representation of the dressed state, the noninteracting Hamiltonian can be expressed as the following form:

$$H_0 = \hbar\Omega R_3 + \hbar\Delta_c a^\dagger a + \hbar\sum_\lambda \Delta_\lambda a_\lambda^\dagger a_\lambda. \tag{11}$$

In the dressed-state basis, the bare atomic operators σ_{12}, σ_{21}, and σ_3 in the H_1, H_2, and $(\partial\rho/\partial t)_{dephase}$ are replaced by the Eqs. (10a) and (10b). Further, we define the time-dependent interaction picture Hamiltonian $\tilde{H}_i = U^\dagger(t)H_iU(t)$, where $U(t) = \exp(-iH_o t/\hbar)$ and $i = 1, 2$. In this interaction picture, the Hamiltonian H_1 and H_2 takes the following form:

$$\tilde{H}_1 = \hbar\chi a^\dagger a^\dagger aa + i\hbar\xi(a^\dagger e^{i(\Delta_c - \Delta_i)t} - ae^{-i(\Delta_c - \Delta_i)t}), \tag{12}$$

$$\begin{aligned}\tilde{H}_2 = {} & i\hbar g(cs\sqrt{a^\dagger a}a^\dagger R_3 e^{i\Delta_c t} + c^2\sqrt{a^\dagger a}a^\dagger R_{12}e^{i(\Delta_c - 2\Omega)t} \\ & - s^2\sqrt{a^\dagger a}a^\dagger R_{21}e^{i(\Delta_c + 2\Omega)t}) + i\hbar\sum_\lambda g_\lambda(sca_\lambda^\dagger R_3 e^{i\Delta_\lambda t} \\ & + c^2 a_\lambda^\dagger R_{12}e^{i(\Delta_\lambda - 2\Omega)t} - s^2 a_\lambda^\dagger R_{21}e^{i(\Delta_\lambda + 2\Omega)t}) + \text{H.c.}\end{aligned} \tag{13}$$

The Hamiltonian $\tilde{H}_1$ keeps the same form even after the unitary transform $U(t)$ is taken, but in the second term, which describes the incident of probing field, the oscillation frequency is changed from Δ_i to $\Delta_c - \Delta_i$. The absolute value of the oscillation frequency has the significant meaning for the secular approximation (in the approximation, the fast oscillating terms will be neglected) [38]. The Hamiltonian $\tilde{H}_2$ describes the nonlinear interaction of the dressed atom with the cavity field and the linear interaction of the dressed atom with the vacuum modes. In Eq. (15), we see that, due to nonlinear defect, the coupling intensity between dressed atom and cavity is also proportional to the amplitude of cavity field. In addition, the characteristic frequencies of oscillation in Eq. (13) are Δ_c and $\Delta_c \pm 2\Omega$. By varying the cavity field detuning Δ_c, we can manipulate the interaction between the driven system and the cavity mode.

Under the Born-Markov approximation [39], by tracing the density operator of the total system over the reservoir variables, the master equation for the reduced density operator of atom plus cavity field system in the dressed-state representation is finally obtained, and after discarding the rapid oscillating terms in the dissipative part, the master equation takes the form

$$\begin{aligned}\frac{\partial\rho}{\partial t} = {} & \frac{1}{i\hbar}[\hbar\chi a^\dagger a^\dagger aa + i\hbar\xi(a^\dagger - a), \rho] \\ & + g(sc[\sqrt{a^\dagger a}a^\dagger R_3 e^{i\Delta_c t} - R_3 a\sqrt{a^\dagger a}e^{-i\Delta_c t}, \rho] \\ & + c^2[\sqrt{a^\dagger a}a^\dagger R_{12}e^{i(\Delta_c - 2\Omega)t} - R_{21}a\sqrt{a^\dagger a}e^{-i(\Delta_c - 2\Omega)t}, \rho] \\ & - s^2[\sqrt{a^\dagger a}a^\dagger R_{12}e^{i(\Delta_c + 2\Omega)t} - R_{12}a\sqrt{a^\dagger a}e^{-i(\Delta_c + 2\Omega)t}, \rho] \\ & + L_A\rho + L_C\rho,\end{aligned} \tag{14}$$

where the superoperators L_A and L_C are defined by

$$\begin{aligned}L_A\rho = {} & \frac{A_0}{2}(R_3\rho R_3 - \rho) + \frac{A_-}{2}(R_{21}\rho R_{12} - R_{12}R_{21}\rho) \\ & + \frac{A_+}{2}(R_{12}\rho R_{21} - R_{21}R_{12}\rho) + \text{H.c.},\end{aligned} \tag{15}$$

$$L_C\rho = \kappa(2a\rho a^\dagger - a^\dagger a\rho - \rho a^\dagger a). \tag{16}$$

Equation (15) describes the spontaneous emission from the dressed atom to the modes of the photonic-crystal radiation reservoir and the Eq. (16) describes the damping of the cavity mode via cavity decay. In Eq. (15), $A_0 = \gamma_0 c^2 s^2 + \gamma_p(c^2 - s^2)$, $A_- = \gamma_- s^4 + 4\gamma_p c^2 s^2$, and $A_+ = \gamma_+ s^4 + 4\gamma_p c^2 s^2$. The spontaneous emission decay rates $\gamma_0 = 2\pi\Sigma_\lambda g_\lambda^2\delta(\omega_\lambda - \omega_L)$, $\gamma_- = 2\pi\Sigma_\lambda g_\lambda^2\delta(\omega_\lambda - \omega_L + 2\Omega)$, and $\gamma_+ = 2\pi\Sigma_\lambda g_\lambda^2\delta(\omega_\lambda - \omega_L - 2\Omega)$ are proportional to the photonic DOS at the dressed-state transition frequencies ω_L and $\omega_L \pm 2\Omega$ [40].

We consider here the case of the cavity field tuned to resonance with the Mollow high-frequency sideband, corresponding to $\Delta_c = 2\Omega$; with the probing field frequency resonance with the cavity field, it means that $\Delta_i = \Delta_c = 2\Omega$. We note that for the optical cavities, the wavelength of the probing field is in the optical domain. The photonic DOS of photonic-crystal radiation reservoir as a function of frequency exists in a discontinuity near a band-edge frequency

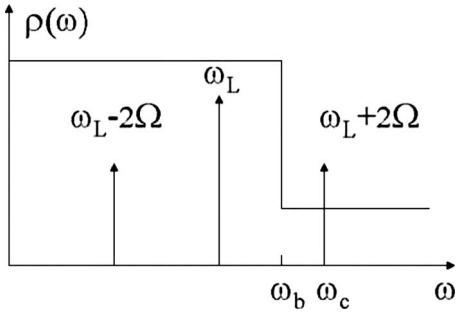

FIG. 2. The relative positions of the relevant frequencies considered in our study. ω_L and ω_c are the coherent pump field frequency and the cavity mode frequency, respectively. $\omega_L \pm 2\Omega$ describes the sideband components of the Mollow spectrum (Ω is the generalized Rabi frequency) and ω_b is the photonic band-edge frequency.

ω_b, exhibits the relevant frequencies for this study, and their relative position are presented in Fig. 2. And then, assuming a strong pump field $\Omega \gg \gamma, \kappa$, one can invoke the secular approximation [38] to ignore the rapidly oscillating terms at frequencies 2Ω and 4Ω in the master equation. In this case, the master equation reduces to

$$\frac{\partial \rho}{\partial t} = \frac{1}{i\hbar}[\hbar\chi a^\dagger a^\dagger aa + i\hbar\xi(a^\dagger - a), \rho] + g_1[\sqrt{a^\dagger a}a^\dagger R_{12} - R_{21}a\sqrt{a^\dagger a}, \rho] + L_A\rho + L_C\rho, \quad (17)$$

where $g_1 = gc^2$ is the effective coupling constant.

In order to derive the bistable states equation of system, we have transformed Eq. (17) into the Schrödinger picture. By this way, we obtain the following master equation:

$$\frac{\partial \rho}{\partial t} = \frac{1}{i\hbar}[\hbar\Omega R_3 + \hbar\Delta_c a^\dagger a + \hbar\chi a^\dagger a^\dagger aa + i\hbar(\zeta a^\dagger - \zeta^* a), \rho] + g_1[\sqrt{a^\dagger a}a^\dagger R_{12} - R_{21}a\sqrt{a^\dagger a}, \rho] + L_A\rho + L_C\rho, \quad (18)$$

where $\zeta = \xi e^{-2i\Omega t}$ and obviously $|\zeta| = |\xi|$.

III. EQUATIONS OF MOTION AND BISTABLE STATES EQUATION

In this section, we derive the bistable states equation of the system. The concept of optical bistability is that there are two output light intensities for single input light intensity when the light pass through certain optical medium, i.e., output light intensity is a nonlinear function of input light intensity [1]. In order to investigate the properties of optical bistability, we have to derive the intensity relation between input light and output light analytically or numerically. This relationship is so-called bistable states equation. For the system under consideration, it is necessary to derive the relation between probing field Rabi frequency and cavity field amplitude. The system is described by reduced density operator ρ consisting of dressed atom plus cavity field and the master equation Eq. (18) enables us to derive equations of motion for expectation values of atomic and cavity field operators. By the fact that $a^\dagger$, a, R_{12}, R_{21}, and R_3 are time-independent Schrödinger picture operators, the equation of motion for their expectation values follows from $\partial\rho/\partial t$ in the master equation. The following sets of equations of motion for the expectation values of various operators are obtained:

$$\frac{d}{dt}\langle a\rangle = -i\Delta_c\langle a\rangle - 2i\chi\langle a^\dagger aa\rangle + g_1\langle\sqrt{a^\dagger a}R_{12}\rangle - \kappa\langle a\rangle + \zeta, \quad (19a)$$

$$\frac{d}{dt}\langle R_{12}\rangle = -2i\Omega\langle R_{12}\rangle - \left(2A_0 + \frac{\gamma_1}{2}\right)\langle R_{12}\rangle + g_1\langle a\sqrt{a^\dagger a}R_3\rangle, \quad (19b)$$

$$\frac{d}{dt}\langle R_3\rangle = -2g_1(\langle\sqrt{a^\dagger a}aa^\dagger R_{12}\rangle + \langle a\sqrt{a^\dagger a}R_{21}\rangle) - \gamma_2 - \gamma_1\langle R_3\rangle. \quad (19c)$$

Equations of $\langle R_{21}\rangle$ and $\langle a^\dagger\rangle$ are the Hermitian conjugates of Eqs. (19a) and (19b). Here we treat $\sqrt{a^\dagger a}$ as a c number in calculating commutation relation and the parameters $\gamma_1 = \gamma_+c^4 + \gamma_-s^4$ and $\gamma_2 = \gamma_+c^4 - \gamma_-s^4$.

Some of the terms in Eqs. (19) contain expectation value of product of the operators. The system of equations will be endless if we continue deriving the equations of motion for their expectation values because we can find that those equations also contain expectation values of more operator products. Consequently, we employ approximation approach. In the following, we neglect the correlation between expectation values of operators, assuming that the expectation values of the product of operators are equal to the product of the expectation values of operators. For the sake of notational simplicity, we introduce a set of complex number α, α^*, S_{12}, S_{21}, and S_3 which indicate the expectation value of operators $\langle a^\dagger\rangle = \alpha^*$, $\langle a\rangle = \alpha$, $\langle R_{12}\rangle = S_{12}$, $\langle R_{21}\rangle = S_{21}$, and $\langle R_3\rangle = S_3$. Then we find the following closed set of nonlinear equations of motion:

$$\frac{d\alpha}{dt} = -i(2\Omega + 2\chi|\alpha|^2)\alpha - \kappa\alpha + g_1S_{12}|\alpha| + \zeta, \quad (20a)$$

$$\frac{d\alpha^*}{dt} = i(2\Omega + 2\chi|\alpha|^2)\alpha^* - \kappa\alpha^* + g_1S_{21}|\alpha| + \zeta^*, \quad (20b)$$

$$\frac{dS_{12}}{dt} = -2i\Omega S_{12} - \left(2A_0 + \frac{\gamma_1}{2}\right)S_{12} + g_1|\alpha|\alpha S_3, \quad (20c)$$

$$\frac{dS_{21}}{dt} = 2i\Omega S_{21} - \left(2A_0 + \frac{\gamma_1}{2}\right)S_{21} + g_1|\alpha|\alpha^* S_3, \quad (20d)$$

$$\frac{dS_3}{dt} = -2g_1|\alpha|(\alpha^* S_{12} + \alpha S_{21}) - \gamma_2 - \gamma_1 S_3. \quad (20e)$$

Equations (20) can be obtained by the following different processes [41]. First, the master equation Eq. (18) can be converted to Fokker-Planck equation by introducing the positive P representation and then using Ito rules to convert this Fokker-Planck equation into stochastic differential equa-

tions. Second, discarding the fluctuation forces in those stochastic differential equations, we can get Eqs. (20) again. Therefore, we can conclude that the approximation employed to derive Eqs. (20) is equivalent to the small fluctuation approximation (i.e., neglecting the fluctuation forces). We focus on the steady solutions of the system. Let the time derivative on the left side of Eqs. (20) equal zero. We obtain a system of algebraic equations

$$-i(2\Omega+2\chi|\alpha|^2)\alpha-\kappa\alpha+g_1S_{12}|\alpha|+\zeta=0, \tag{21a}$$

$$i(2\Omega+2\chi|\alpha|^2)\alpha^*-\kappa\alpha^*+g_1S_{21}|\alpha|+\zeta^*=0, \tag{21b}$$

$$-2i\Omega S_{12}-\left(2A_0+\frac{\gamma_1}{2}\right)S_{12}+g_1|\alpha|\alpha S_3=0, \tag{21c}$$

$$2i\Omega S_{21}-\left(2A_0+\frac{\gamma_1}{2}\right)S_{21}+g_1|\alpha|\alpha^* S_3=0, \tag{21d}$$

$$-2g_1|\alpha|(\alpha^* S_{12}+\alpha S_{21})-\gamma_2-\gamma_1 S_3=0. \tag{21e}$$

After some algebra, we have

$$\zeta=\alpha\left[\left(\kappa+\frac{g_1^2|\alpha|^2\gamma_2\gamma_\perp}{4g_1^2|\alpha|^4\gamma_\perp+\gamma_1(4\Omega^2+\gamma_\perp^2)}\right)+i\left(2\Omega+2\chi|\alpha|^2-\frac{2\Omega g_1^2|\alpha|^2\gamma_2}{4g_1^2|\alpha|^4\gamma_\perp+\gamma_1(4\Omega^4+\gamma_\perp^2)}\right)\right]. \tag{22}$$

Here, $\gamma_\perp=2A_0+\gamma_1/2$. Equation (22) is the bistable states equation of the system.

IV. OPTICAL BISTABILITY IN THE CAVITY

In this section, we discuss the dependence of bistability on the PBG of the photonic crystal, driving field Rabi frequency and dephasing processes. As we have already mentioned, we work in the strong-coupling regime

$$g \gg \gamma,\kappa. \tag{23}$$

This condition is satisfied in a typical band-gap material. For example, one can take the atomic transition frequency and the pumping field frequency and as $\omega_a\approx\omega_L\approx10^{15}$ Hz, the electric-dipole moment of an atom $d_{21}\approx10^{-29}$ Cm, and the cavity mode volume of $V\approx10^{-6}$ m^3, then the atom cavity coupling will be $g\approx10^{10}$ Hz [29,42]. For a spontaneous emission decay rate in a free space of $\gamma=10^8$ Hz, $\gamma_-=100\gamma$ and quality factor Q of 10^6 corresponds to a cavity decay rate $\kappa\approx10^9$ Hz. For a frequency detuning $|\Delta_a|\approx10^{-7}\omega_a$ in the optical regime, the value of pumping Rabi frequency used in the calculations corresponds to the electric field amplitude $E\approx10^3$ V/m [26]. Thus the inequality Eq. (23) is easy satisfied. In experimental design, one can select doped semiconductor CdS_xSe_{1-x} glass as materials, which has large nonlinear refractive index coefficient and very short nonlinear responding time, to compose point defect in photonic crystal. Moreover, the photonic-crystal microcavity architecture can be realized by embedding a dielectric microcavity (defect) within a two-mode waveguide channel in a two-dimensional (2D) PBG microchip [26]. One mode of the waveguide channel is engineered to produce a large discontinuity in the local photon density of states near the atom and another mode is used to propagate the pump-laser beam. By suitable engineering, it is possible to realize a strong coupling of the atom to both the pumping waveguide mode and the high-Q cavity mode [26]. The physical parameters of such photonic-crystal architecture was proposed and discussed in detail in Ref. [26]. We note that for the optical cavities, the wavelength of the probing field is about $10^{-3}-10^3$ μm.

For simplicity, we introduce new dimensionless parameters $n_0=\gamma_2\gamma_\perp/(4g_1^2)$, $x=|\alpha|/\sqrt{n_0}$, $y=|\zeta|/(\kappa\sqrt{n_0})$, $r=\gamma_+/\gamma_-$, $C=g_1^2/(2\kappa\gamma_\perp)$, $\eta=\chi/\kappa$, $R=\gamma_1/\gamma_2$, $\Sigma_1=2\Omega/\kappa$, and $\Sigma_2=2\Omega/\gamma_\perp$, where y is the normalized input intensity and x is the normalized cavity field amplitude. r describes the size of the discontinuity on the photonic DOS under the situation of a full PBG with no radiation mode for the high Mollow sideband $r=\gamma_+/\gamma_-=0$ and $r=\gamma_+/\gamma_-=1$ for the free-space case.

Equation (22) can be written in the following form:

$$|y|^2=|x|^2\left[\left(1+\frac{2C|x|^2}{|x|^4+R\dfrac{\Sigma_2^2+1}{n_0}}\right)^2+\left(\Sigma_1+2n_0\eta|x|^2-\frac{2C|x|^2\Sigma_2}{|x|^4+R\dfrac{\Sigma_2^2+1}{n_0}}\right)^2\right]. \tag{24}$$

In the following, we will employ Eq. (24) to discuss the bistability of the system. For simplicity, we take $\gamma_p=0$ (i.e., neglecting the dipolar dephase), $\kappa=0.1\gamma_-$ (i.e., in the good cavity limit), and $\chi/\kappa=0.5$. In a strong-coupling regime ($g=10\kappa$), we take the driving field intensity as $\varepsilon/|\Delta_a|=0.75$ for the negative detuning ($\Delta_a<0$) between the atomic resonant frequency and driving field frequency.

Figure 3 presents the normalized cavity field amplitude as a function of the normalized incident probing field intensity for the cavity in ordinary vacuum ($r=1$). In Fig. 3, the typical S-shaped response indicates that the system can exhibit a bistability. The point H denotes the high threshold value U_H of the probing field intensity and L denotes the low threshold value U_L. The hysteresis cycle width ΔU is defined by

$$\Delta U=U_H-U_L. \tag{25}$$

The curve in Fig. 3 means that when the incident intensity increases to the point H, the cavity field amplitude suddenly becomes a very large value. However, as the incident intensity decreases to the point L, the cavity field amplitude jumps into a very small value. As a result, a hysteresis cycle is formed in Fig. 3. One can find that the system has two stable branches [1] in the two sides of S-shape curve, where the derivative of cavity field amplitude x with respect to the probing field amplitude y is greater than zero (i.e., $dx/dy>0$). However, the middle part of S-shape curve, where $dx/dy<0$, corresponds to the unstable branch of the system.

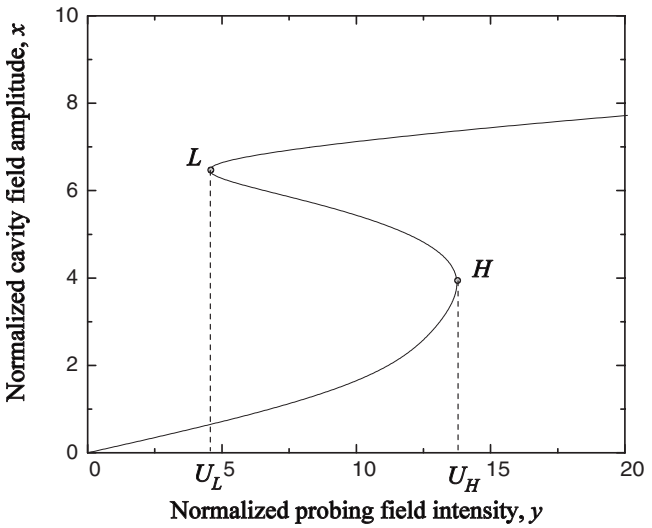

FIG. 3. The normalized cavity field amplitude in the absence of dipolar dephasing as a function of the normalized probing field intensity for negative detuning between the atomic resonant frequency and the driving field frequency $\Delta_a<0$. We have set $\kappa=0.1\gamma_-$, $g=10\kappa$, $\chi=0.5\kappa$, and the cavity is imbedded in the ordinary vacuum (i.e., $r=1$), the scaled driving field Rabi frequency $\varepsilon/|\Delta_a|=0.75$ in the calculation.

If the cavity field intensity is in the unstable branch initially, it may jump to the stable branches when there is a perturbation to the probing intensity. Thus, when the probing field intensity belongs to the interval $[U_L, U_H]$, the system can exhibit a bistability. The normalized incident intensity values of point $H(L)$ correspond to 13.78 (4.19).

In order to demonstrate the controllability of the optical bistability, we present in Fig. 4 the normalized cavity field amplitude as a function of the normalized probing field intensity for various values of the discontinuity in the photonic DOS. The magnitude of the jump in photonic DOS ranges from the case of a cavity engineered in a photonic crystal with a full PBG (i.e., $r=0$) to the case of a cavity in ordinary vacuum (i.e., $r=1$) and other parameters are the same as those in Fig. 3. The insert figure in Fig. 4 presents the curve of $r=0.1$. We can see that the high threshold value increases with the increasing of the discontinuity of photonic DOS, but the low threshold value keeps unchanged basically. This tendency means the hysteresis cycle width will be enlarged when photonic DOS jump between the Mollow spectral components is large. For a cavity engineered in a photonic crystal with a full PBG, the curve cannot be retraced to perform an S shape for any input intensities. In this case, the cavity field amplitude is a linear function of probing field intensity and the bistability of the cavity field vanishes. We depict the dependence of U_H, U_L, and ΔU on the discontinuity in photonic DOS in Fig. 5. The hysteresis cycle width and high threshold value also increase with increasing of pumping field intensity as presented in Fig. 6. Here we alter the pumping field Rabi frequency from $\varepsilon/|\Delta_a|=0.25$ to $\varepsilon/|\Delta_a|=1$ and fix the jump of photonic DOS at $r=0.8$. The other parameters are the same as those given in Fig. 3. As shown above, we can conclude that the effect of the adjustment to physical parameter of the one-atom laser in photonic-crystal

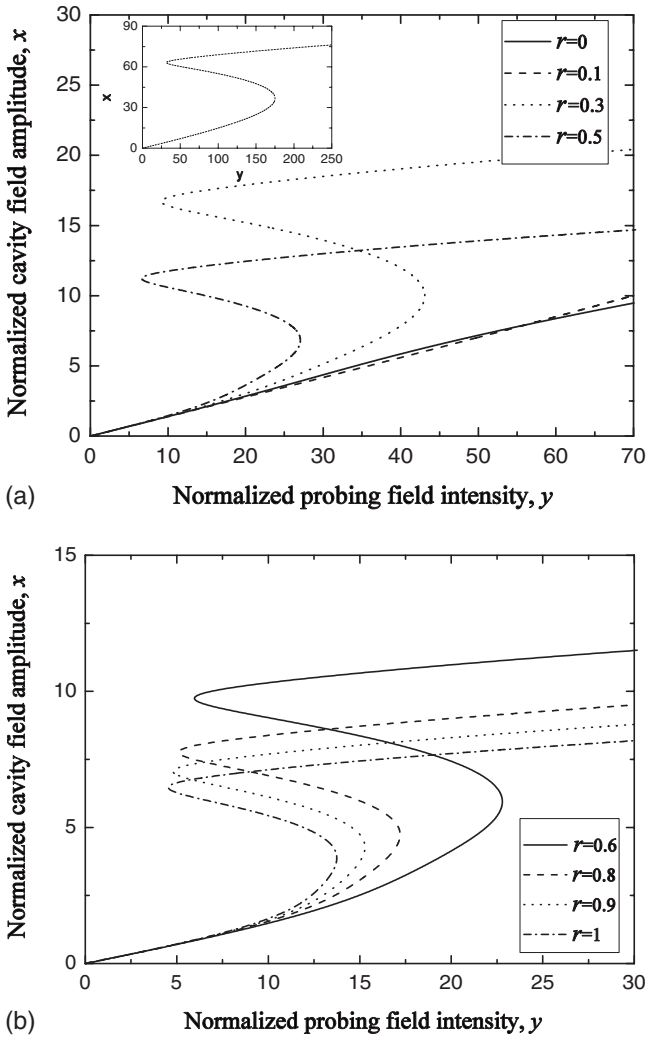

FIG. 4. The normalized cavity field amplitude in the absence of dipolar dephasing as a function of the normalized probing field intensity for negative detuning between the atomic resonant frequency and the driving field frequency $\Delta_a<0$ and for various values of the jump in photonic DOS. We have set $\kappa=0.1\gamma_-$, $g=10\kappa$, $\chi=0.5\kappa$, and the scaled driving field Rabi frequency $\varepsilon/|\Delta_a|=0.75$ in the calculations. (a) $r=0,0.1,0.3,0.5$. (b) $r=0.6,0.8,0.9,1$. Insert shows the curve of $r=0.1$.

microcavity is equivalent to the indirect modulation of the nonlinear coefficient of the nonlinear defect.

The reason for the above results can be qualitatively explained as follows. It is well known that photonic band structure can manipulate atom-emitting photons to cavity mode. The atom spontaneous emission, which leads to emission of photons into the reservoir modes different from the cavity mode, can be reduced when the photonic DOS jump between the Mollow spectral components is large. As a result, the process of stimulated emission into the cavity mode dominates the total process of atom-emitting photons. Therefore, the cavity photon number is enhanced for large discontinuities in the photonic DOS (i.e., small value of r). In Eq. (4), the strength of the coupling between atom and cavity mode is proportional to the amplitude of cavity field because of the existence of nonlinear material in the cavity. Therefore, the

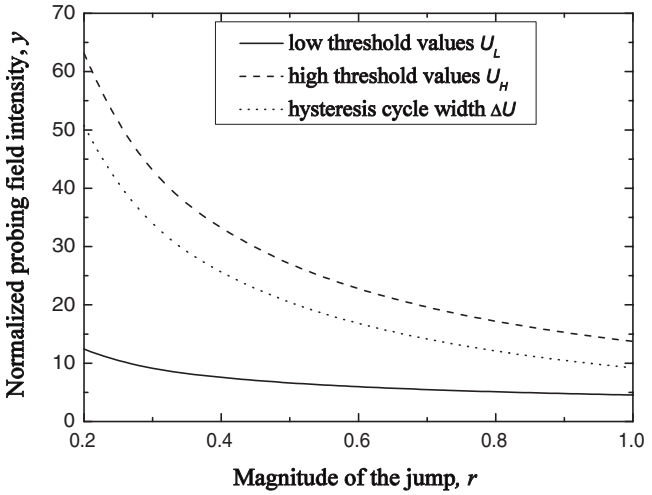

FIG. 5. The influence of the discontinuity of photonic DOS on hysteresis cycle width, high and low threshold values, in the absence of dipolar dephasing for negative detuning between the atomic resonant frequency and the driving field frequency $\Delta_a<0$. We have set $\kappa=0.1\gamma_-$, $g=10\kappa$, $\chi=0.5\kappa$, and the scaled driving field Rabi frequency $\varepsilon/|\Delta_a|=0.75$ in the calculations.

increase of photon number in cavity is equivalent to enhance the coupling between atom and cavity field. Consequently, it favors to the energy transmission between the atomic system and the cavity field. When the input intensity is increased, more photons will enter the cavity mode and the energy will be transferred from the cavity field to atom quite easily. As a result, the stronger incident intensity is needed in order to make cavity field saturation. Therefore, both the cavity field amplitude and high threshold value increases. If the input is reduced, the distributed feedback mechanism enables the system to retain a sufficiently large internal cavity field intensity so that the output intensity is maintained. The input

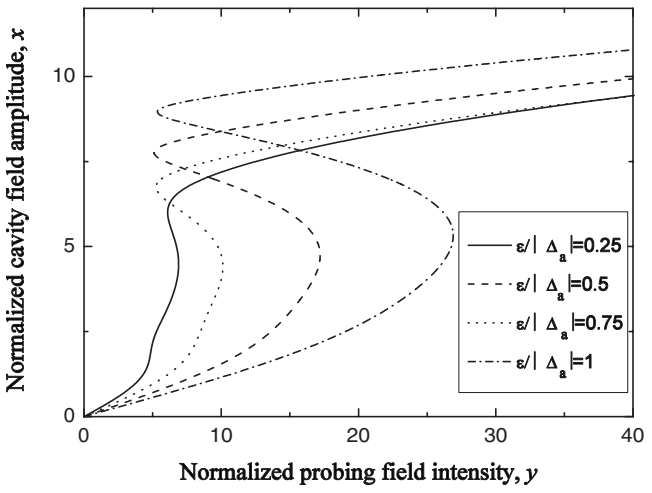

FIG. 6. The normalized cavity field amplitude in the absence of dipolar dephasing as a function of the normalized probing field intensity for various values of the scaled driving field Rabi frequency $\varepsilon/|\Delta_a|$ and for negative detuning between the atomic resonant frequency and the driving field frequency $\Delta_a<0$. We have set $\kappa=0.1\gamma_-$, $g=10\kappa$, $\chi=0.5\kappa$, and $r=\gamma_+/\gamma_-=0.8$ in the calculations.

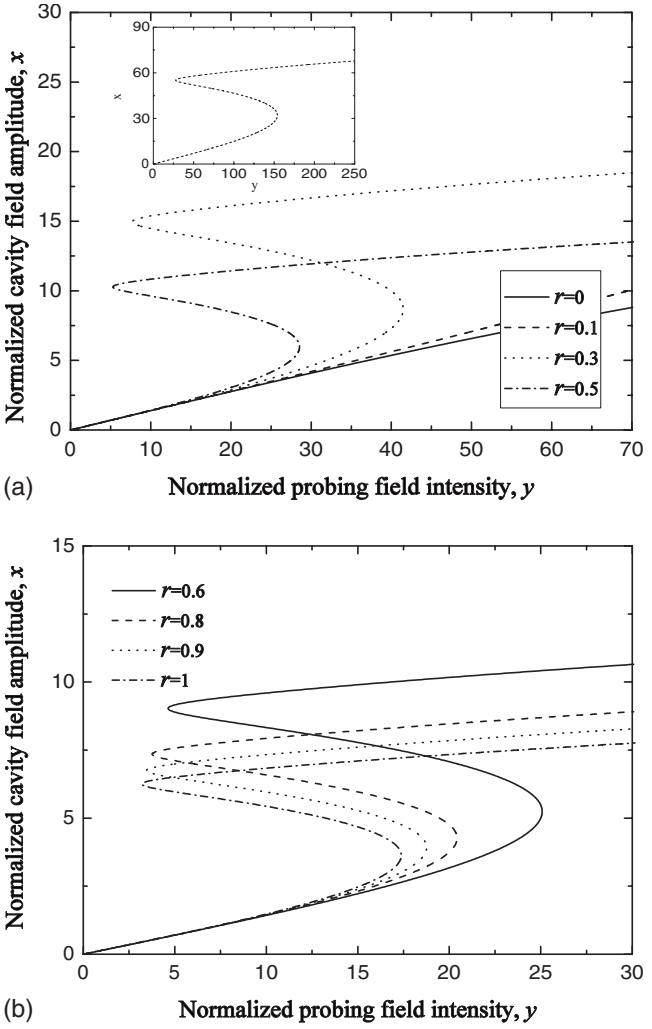

FIG. 7. The normalized cavity field amplitude in the presence of dipolar dephasing as a function of the normalized probing field intensity for negative detuning between the atomic resonant frequency and the driving field frequency $\Delta_a<0$ and for various values of the jump in photonic DOS. We have set $\kappa=0.1\gamma_-$, $g=10\kappa$, $\chi=0.5\kappa$, $\gamma_p=0.1\kappa$, and the scaled driving field Rabi frequency $\varepsilon/|\Delta_a|=0.75$ in the calculations. (a) $r=0,0.1,0.3,0.5$. (b) $r=0.6,0.8,0.9,1$. Insert shows the curve of $r=0.1$.

has to drop below the original switch-up intensity before the cavity falls to a low value. The hysteretic curve was shown in Figs. 3 and 4.

We now investigate the effect of additional dephasing on the bistability characteristics. In Fig. 7, we plot the normalized amplitude of the cavity field as a function of the normalized probing field intensity when an addition dephasing is present in the system ($\gamma_p=0.1\kappa$), where all the physical parameters are the same as those in Fig. 4. The insert figure in Fig. 7 presents the curve of $r=0.1$. Compared to Fig. 4, we note that the high threshold value in Fig. 7 is larger and the region of bistability is increased slightly. Those tendencies are accompanied by the little decrease of the cavity field intensity of two stable states in the same magnitude of discontinuity in the photonic DOS. To understand the characteristics mentioned above, one needs to recall that the dipolar dephasing can transfer the atom from a dressed state to an-

other dressed state without the emission of a photon. As a result, for the same probing field intensity, the cavity field amplitude is lower than the case when no dipolar dephasing is present (see Fig. 4). Moreover, the higher incident intensity is needed in order to make cavity field saturation, i.e., the high threshold values are increased. From Fig. 7, we can conclude that despite the dephasing processes have a deleterious effect on the photon emission [27], but in our case, the effect of dephasing processes on bistable characteristics is insignificant.

V. SUMMARY

We investigate the property of bistability of cavity field amplitude in a photonic-crystal one-atom laser when the microcavity is considered to be fabricated by nonlinear material. We have considered the case of the microcavity frequency tuned on resonance with one of the sidebands of Mollow atomic resonance fluorescence spectrum and the probing field frequency resonance with the microcavity. Under certain conditions, the cavity field exhibits bistability. When the discontinuity in the photonic density of states increases, the high threshold value and the cavity field amplitude will also increase and so will the hysteresis cycle width. If the microcavity resonance occurs in a full photonic band gap, the bistability vanishes whatever other parameters are. In addition, the increase of Rabi frequency of pumping field will also lead to the enlargement of the hysteresis cycle width. The bistable behavior vanished as the pumping field Rabi frequency was decreased. When the additional dephasing is taken into account, the hysteresis cycle width will enlarge insignificantly. But the general bistable characteristics will keep unchanged. Those results clearly illustrate the ability to control optical bistability through suitable photonic-crystal architectures and external coherent driving field instead of adjusting the nonlinear materials and this study suggests that in a photonic-crystal nonlinear microcavity, the one-atom laser acts as an effective controllable bistable device in the design of all-light digital computing systems in the near future.

ACKNOWLEDGMENTS

The authors acknowledge financial support from the Creative Foundation of the Heilongjiang Province of China (Grant No. YJSCX2009-255HLJ), the Predict Project for the Development of Science and Technology of Harbin Normal University (Grant No. 08XYG-02), and the Natural Science Foundation of the Heilongjiang Province of China (Grant No. A200812). X.Y.G. thanks M. Sc. Zi-meng Chi for her helpful advice.

[1] H. M. Gibbs, *Optical Bistability: Controlling Light with Light* (Academic, New York, 1985).
[2] R. Z. Wang, J. M. Dong, and D. Y. Xing, Phys. Rev. E **55**, 6301 (1997).
[3] J. Danckaert, K. Fobelets, I. Veretennicoff, G. Vitrant, and R. Reinisch, Phys. Rev. B **44**, 8214 (1991).
[4] J. He and M. Cada, IEEE J. Quantum Electron. **27**, 1182 (1991).
[5] E. Wolf, *Progress in Optics* (North-Holland Physics Publishing, Amsterdam, 1984).
[6] V. M. Agranovich, S. A. Kiselev, and D. L. Mills, Phys. Rev. B **44**, 10917 (1991).
[7] M. Soljačić, M. Ibanescu, S. G. Johnson, J. D. Joannopoulos, and Y. Fink, Opt. Lett. **28**, 516 (2003).
[8] M. F. Yanik, S. Fan, M. Solčić, and J. D. Joannopoulos, Opt. Lett. **28**, 2506 (2003).
[9] C. P. Liu, S. Q. Gong, X. J. Fan, and Z. Z. Xu, Opt. Commun. **231**, 289 (2004).
[10] C. P. Liu, S. Q. Gong, X. J. Fan, and Z. Z. Xu, Opt. Commun. **239**, 383 (2004).
[11] W. J. Jiang, X. Yan, J. P. Song, H. B. Zheng, C. Wu, B. Y. Yin, and Y. Zhang, Opt. Commun. **282**, 101 (2009).
[12] M. Chen, C. F. Li, M. Xu, W. B. Wang, Y. X. Xia, and S. J. Ma, Opt. Commun. **255**, 46 (2005).
[13] P. Hou, Y. Chen, J. Shi, M. Shen, and Q. Wang, Opt. Commun. **273**, 441 (2007).
[14] R. R. Wei, X. Chen, J. W. Tao, and C. F. Li, Phys. Lett. A **372**, 6797 (2008).
[15] J. Zakrzewski, M. Lewenstein, and T. W. Mossberg, Phys. Rev. A **44**, 7717 (1991).
[16] M. Lewenstein, Y. Zhu, and T. W. Mossberg, Phys. Rev. Lett. **64**, 3131 (1990).
[17] M. Loffler, G. M. Meyer, and H. Walther, Phys. Rev. A **55**, 3923 (1997).
[18] P. Lougovski, F. Casagrande, A. Lulli, and E. Solano, Phys. Rev. A **76**, 033802 (2007).
[19] H. J. Kim, A. H. Khosa, H. W. Lee, and M. S. Zubairy, Phys. Rev. A **77**, 023817 (2008).
[20] E. Yablonovitch, Phys. Rev. Lett. **58**, 2059 (1987).
[21] S. John and J. Wang, Phys. Rev. Lett. **64**, 2418 (1990).
[22] S. John and T. Quang, Phys. Rev. A **50**, 1764 (1994).
[23] T. Quang, M. Woldeyohannes, S. John, and G. S. Agarwal, Phys. Rev. Lett. **79**, 5238 (1997).
[24] S. John and T. Quang, Phys. Rev. Lett. **78**, 1888 (1997); S. John and M. Florescu, J. Opt. A, Pure Appl. Opt. **3**, S103 (2001).
[25] S. John, Phys. Rev. Lett. **58**, 2486 (1987).
[26] L. Florescu, S. John, T. Quang, and R. Wang, Phys. Rev. A **69**, 013816 (2004).
[27] L. Florescu, Phys. Rev. A **74**, 063828 (2006).
[28] L. Florescu, Phys. Rev. A **78**, 023827 (2008).
[29] R. Tan, G. X. Li, and Z. Ficek, Phys. Rev. A **78**, 023833 (2008).
[30] D. Englund, D. Fattal, E. Waks, G. Solomon, B. Zhang, T. Nakaoka, Y. Arakawa, Y. Yamamoto, and J. Vuckovic, Phys. Rev. Lett. **95**, 013904 (2005).
[31] A. Badolato *et al.*, Science **308**, 1158 (2005).
[32] S. Strauf, K. Hennessy, M. T. Rakher, Y. S. Choi, A. Badolato,

L. C. Andreani, E. L. Hu, P. M. Petroff, and D. Bouwmeester, Phys. Rev. Lett. **96**, 127404 (2006).
[33] M. Deubel, M. Wegener, S. Linden, G. Von Freymann, and S. John, Opt. Lett. **31**, 805 (2006).
[34] A. Chutinan, S. John, and O. Toader, Phys. Rev. Lett. **90**, 123901 (2003); A. Chutinan and S. John, Phys. Rev. E **71**, 026605 (2005).
[35] A. Joshi and R. R. Puri, Phys. Rev. A **45**, 5056 (1992).
[36] M. Florescu and S. John, Phys. Rev. A **69**, 053810 (2004).
[37] A. D. Greentree, J. Salzman, S. Prawer, and L. C. L. Hollenberg, Phys. Rev. A **73**, 013818 (2006).
[38] G. S. Agarwal, L. M. Narducci, D. H. Feng, and R. Gilmore, Phys. Rev. Lett. **42**, 1260 (1979).
[39] H. J. Carmichael, *Statistical Methods in Quantum Optics I* (Springer-Verlag, Berlin, 1999).
[40] B. R. Mollow, Phys. Rev. A **5**, 2217 (1972).
[41] C. W. Gardiner, *Handbook of Stochastic Process* (Springer, Berlin, 1984).
[42] M. Florescu and S. John, Phys. Rev. A **64**, 033801 (2001).